



Volcanic Plume Elevation Model and its velocity derived from Landsat 8



Marcello de Michele*, Daniel Raucoules, Þórður Arason

Natural Risks Department, French Geological Survey, 45000 Orleans, France
Icelandic Meteorological Office, Reykjavik, Iceland

ARTICLE INFO

Article history:

Received 24 August 2015
Received in revised form 27 November 2015
Accepted 28 January 2016
Available online xxxx

Keywords:

Volcanic plume
Elevation model
Landsat 8
Holuhraun

ABSTRACT

In this paper we present a method to reconstitute the volcanic gas/ash Plume Elevation Model (PEM) from optical satellite imagery. As the volcanic plume is moving rapidly, conventional satellite based photogrammetric height restitution methods do not apply as the epipolar offset due to plume motion adds up to the one generated by the stereoscopic view. This is because there are time-lags of tens of seconds between conventional satellite stereoscopic acquisitions, depending on the stereo acquisition mode. Our method is based on a single satellite pass. We exploit the short time lag and resulting baseline that exist between the multispectral (MS) and the panchromatic (PAN) bands to jointly measure the epipolar offsets and the perpendicular to the epipolar (P2E) offsets. The first are proportional to plume height plus the offsets due to plume velocity in the epipolar direction. The second, are proportional to plume velocity in the P2E direction only. The latter is used to compensate the effect of plume velocity in the stereoscopic offsets by projecting it on the epipolar direction assuming a known plume direction, thus improving the height measurement precision. We apply the method to Landsat 8 data taking into account the specificities of the focal plane modules. We focus on the Holuhraun 2014 fissure eruption (Iceland). We validate our measurements against ground based measurements. The method has potential for detailed high resolution routine measurements of volcanic plume height/velocity. The method can be applied both to other multifocal plane modules push broom sensors (such as the ESA Sentinel 2) and potentially to other push-broom systems such as the CNES SPOT family and Pléiades.

© 2016 Elsevier Inc. All rights reserved.

1. Introduction

1.1. Importance

The retrieval of both height and velocity of a plume is an important issue in volcanology. As an example, it is known that large volcanic eruptions can temporarily alter the climate, causing global cooling and shifting precipitation patterns (e.g. Robock, 2000); the ash/gas dispersion in the atmosphere, their impact and lifetime around the globe, greatly depends on the injection altitude. Plume height information is critical for ash dispersion modelling and air traffic security. Furthermore, plume height during explosive volcanism is the primary parameter for estimating mass eruption rate (e.g. Mastin et al., 2009). Knowing the plume altitude is also important to get the correct amount of SO₂ concentration from dedicated spaceborne spectrometers (e.g. Carboni, Grainger, Walker, Dudhia, & Siddans, 2012; Corradini, Merucci, Prata, & Piscini, 2010). Moreover, the distribution of ash deposits on ground greatly depends on the ash cloud altitude, which has an impact on risk assessment and crisis management. Furthermore, a spatially detailed plume height measure could be used as a hint for gas emission rate estimation and for ash plume volume researches, which both have an

impact on climate research, air quality assessment for aviation and finally for the understanding of the volcanic system itself as ash/gas emission rates are related to the state of pressurization of the magmatic chamber (e.g. Hreinsdottir et al., 2014; Urai, 2004). Today, the community mainly relies on ground based measurements (e.g. Arason, Petersen, & Bjornsson, 2011; Petersen, Bjornsson, Arason, & von Löwis, 2012; Scollo et al., 2014) but often they can be difficult to collect as by definition volcanic areas are dangerous areas (presence of toxic gases) and can be remotely situated and difficult to access. Satellite remote sensing offers a comprehensive and safe way to estimate plume height. The various techniques that can be used today either estimate average volcanic plume heights indirectly, based on wind speed for instance (see Sparks et al., 1997 for a review) or plume shadowing (e.g. Simpson, McIntire, Jin, & Stitt, 2000; Spinetti et al., 2013), each of which do not aim at restituting a spatially detailed map of the plume heights. Conventional photogrammetric restitution based on satellite imagery fails in precisely retrieving a Plume Elevation Model as the plume own velocity induces an apparent parallax that adds up to the standard parallax given by the stereoscopic view. Therefore, measurements based on standard satellite photogrammetric restitution do not apply as there is an ambiguity in the measurement of the plume position. Standard spaceborne along-track stereo imagers (e.g. SPOT 5, ASTER or Quickbird among the others) present a long temporal lag between the two stereo image acquisitions. It can reach tens of seconds

* Corresponding author.

for baseline-to-height ratios (B/H) between 0.2 and 0.5, during which time the surface texture of the plume may have changed due to the plume fast displacement (i.e. velocities larger than 10 m/s) biasing automatic cross correlation offset measurements (Kääb & Leprince, 2014). Urai (2004) succeeded in retrieving the plume height on Miyakejima volcano using ASTER stereoscopic view, on 3 specific points manually chosen on the forward and backward images. However, for the purpose of PEM extraction, the ideal is as small as possible time lag, with still a B/H ratio large enough to provide a stereoscopic view for restituting the height.

1.2. Method

In this study we propose to use the physical distance that exists between the panchromatic band (PAN) and a multispectral band (MS) in push broom spaceborne sensors to jointly measure the plume velocity and its height, at a high spatial resolution. A number of push broom sensors present a physical distance between the PAN and MS bands. This is because the PAN and MS Charge Coupled Devices (CCDs) sensors cannot coexist in an identical position on the focal plane of the instrument. This physical offset between the CCDs yields a baseline (i.e. the distance between the sensor positions when it acquires two images) and a time lag between the PAN and the MS bands acquisitions. On the one hand, the small baseline has already been successfully exploited for retrieving Digital Elevation Models (DEMs) of still surfaces such as topography or building heights (e.g. Mai & Latry, 2009; Massonnet, Giros, & Breton, 1997; Vadon, 2003). On the other hand, the time lag has been successfully exploited to measure the velocity field of moving surfaces, such as ocean waves and arctic river discharges (e. g. de Michele, Leprince, Thiébot, Raucoules, & Binet, 2012; Kääb, Lamare, & Abrams, 2013; Kääb & Leprince, 2014; Poupardin, Idier, de Michele, & Raucoules, 2015). The problem of extracting a spatially detailed elevation model of a moving surface such as a volcanic gas/ash plume has not yet been addressed by common photogrammetric methods. The aim of this paper is to propose a method to address this problem. We propose a method based on a single pass of Landsat 8. We focus on the 2014–2015 Holuhraun fissure eruption (Iceland) as a test case.

The 2014–2015 Holuhraun eruption in the Bárðarbunga volcanic system is the largest fissure eruption in Iceland since the 1783 Laki eruption (Sigmundsson et al., 2015). It started at the end of August 2014 and lasted six months, to late February 2015. It has been characterized by large degassing processes and emission of SO₂ into the atmosphere (Gottelman, Schmidt, & Kristjánsson, 2015; Haddadi,

Moune, Sigmarrsson, Gauthier, & Gouhier, 2015). The eruption steam and gas column was nicely captured by the Landsat 8 on 6 September 2014 at 12:25 UTC (Fig. 1). The reasons why we use Landsat 8 data are manyfold. Firstly, Landsat 8 captured the Holuhraun fissural eruption on a clear sky conditions. Secondly, raw Landsat 8 data are provided free of charge by the United States Geological Survey (USGS). Thirdly, Landsat 8 CCD sensors accommodation on the focal plane is somehow similar to the one employed by the ESA Sentinel-2, which is of high interest for the ash/gas plume research community as Sentinel-2 data will be free of charge and high revisit time. We chose the Holuhraun eruption as it represents a challenging test case for us as its plume was rapidly moving and reached low altitudes. Therefore, if our method works on the Holuhraun test case then it will apply to other types of volcanic plumes (higher and slower).

2. Data

The Landsat 8 Operational Land Imager (OLI) is a push-broom (linear array) imaging system that collects visible, Near-InfraRed (NIR), and Short-Wavelength InfraRed (SWIR) spectral band imagery at 30-m (15-m panchromatic) ground sample distance (Storey, Choate, & Lee, 2014). It collects a 190-km-wide image swath from a 705-km orbital altitude.

The OLI architecture is described as follows by Knight and Kvaran (2014) and Storey et al. (2014). The OLI detectors are distributed across 14 separate Focal Plane Modules (FPMs), each of which covers a portion of the 15-degree OLI cross-track field of view. Adjacent FPMs are offset in the along-track direction to allow for FPM-to-FPM overlap. This is to avoid any gaps in the cross-track coverage. The reader should refer to Fig. 1 in Storey et al. (2014) for the OLI layout image. The important point in this study is that the internal layout of all 14 FPMs is the same, but with alternate FPMs being rotated by 180° to keep the active detector areas as close together as possible. This has the effect of inverting the along-track order of the spectral bands in adjacent FPMs. Such an assembling of FPMs is rather frequent for multi-spectral sensors and is similar to the Sentinel-2 sensor. The OLI can be thought of as being composed of 14 individual sub-sensors, each of which covers approximately 1/14th of the cross-track field of view. Details of the OLI focal plane layout are presented by Knight and Kvaran (2014) and Storey et al. (2014). USGS provide orthorectified Landsat 8 data free of charge and raw data on demand. Our analysis is based on raw data.

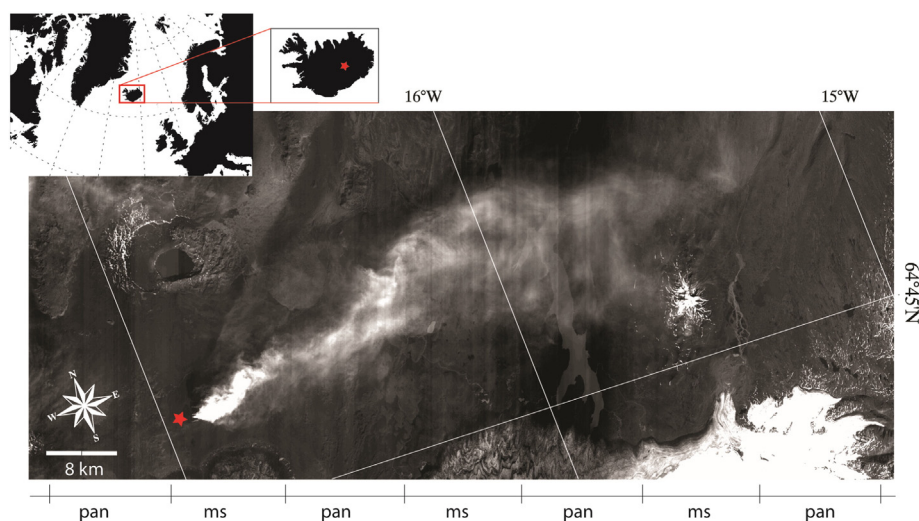


Fig. 1. The study area. Holuhraun (Iceland) eruption site (red star) and the volcanic plume from Landsat 8. The data were acquired on 6 September 2014. We reconstructed this image from raw Landsat data (courtesy of USGS). The image is made of alternate PAN–MS stripes from adjacent FPMs. (For interpretation of the references to colour in this figure legend, the reader is referred to the web version of this article.)

3. Method and results

We exploit both the time lag and the baseline between the PAN and MS image acquisitions. We chose the red channel as the PAN/red time lag is significantly larger than the PAN/blue time lag while the central frequency is closer to the PAN central frequency than the blue channel. The nominal PAN/red time lag is 0.52 s while the nominal angular separation is 0.3° (Jim Storey, pers. Comm.). The platform flies at a nominal altitude of 705 km at a nominal speed of 7.5 km/s. So the base-to-height ratio (B/H) is 0.0055. Alternatively, one might use the green channel instead of the red (which time lag is 0.65 s).

Things are a bit more complicated since the internal layout of all 14 FPMs is the same, but with alternate FPMs being rotated by 180° . When measuring velocities from offsets from cross correlation techniques there will be a sign opposition between velocities measured on adjacent FPMs. To compensate for this, we propose the following approach; from raw data, instead of assembling one PAN image and one MS image, we construct two mixed images. The first is made of alternate PAN–MS bands and the second is made of alternate MS–PAN bands from adjacent FPMs so that the time lag is kept at 0.52 s without sign ambiguity (e.g. Fig 1). The MS data are oversampled to match the PAN spatial resolution of 15 m. Then, we perform offset measurements between the reconstructed images with the standard cross correlation approach (e.g. Leprince, Barbot, Ayoub, & Avouac, 2007) (Fig. 2). We use a correlation window of 32×32 pixel size with 16 pixels sampling interval. This yields a 240 m pixel size offset grid. In a pioneering work, Urai (2004) proposed to use the P2E direction to estimate the wind speed and use

this information to adjust the height estimation on 3 selected pixels belonging to the ash plume. The P2E offsets are independent of height, by definition. Therefore, offsets occurring in the P2E direction would be due to the motion of the observed surface in the P2E direction. By measuring the plume direction (i. e. $\sim 30^\circ$ with respect to the P2E direction) we back-project the P2E offsets on the plume direction to retrieve plume velocity (Fig. 2b). The offsets in the epipolar direction (along track offset, Fig. 2a) are the sum of both a offset component proportional to the plume height and a component proportional to the apparent height due to the plume velocity.

We convert the formerly retrieved plume velocity to apparent height contribution. Finally, we compensate the apparent height contribution on the along track offset to retrieve the PEM (Fig. 3). We start by calculating the pixel offsets due to the plume height only:

$$O_h = O_e - O_{p2e} \tan \theta \quad (1)$$

where O_h is the pixel offset due to the plume height only, O_e is the pixel offset in the epipolar direction, O_{p2e} is the pixel offset in the P2E direction, and θ is the angle between the plume major axis and the columns direction of the image matrix. From O_h we retrieve the PEM by applying (Urai, 2004)

$$h = O_h \cdot s \cdot H / (V \cdot t) \quad (2)$$

where h is the plume height (m), s is the pixel size (m), V is the platform velocity (m/s), t is the temporal lag between the two Landsat-8 bands

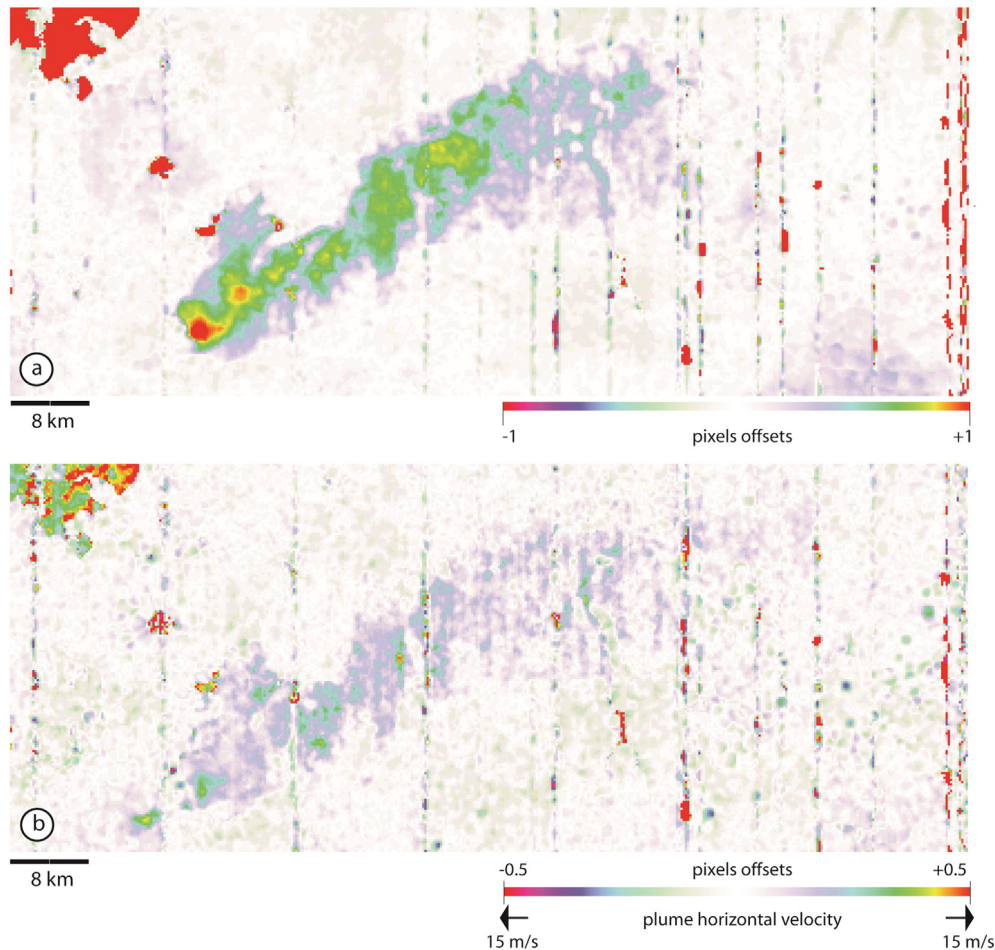


Fig. 2. Pixel offsets from correlation analysis. a) Offsets in the epipolar direction (due both to parallax and plume velocity in the along-track direction). b) P2E offset (due to horizontal plume velocity in the P2E direction).

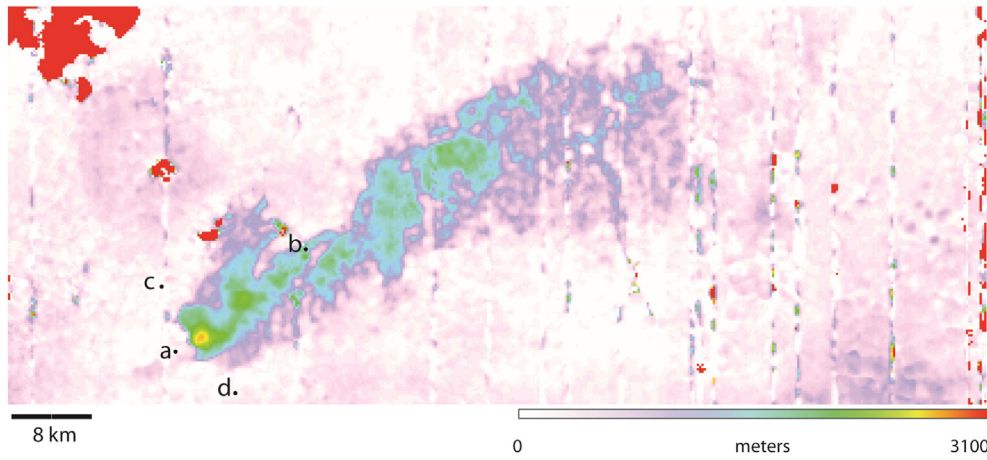


Fig. 3. The Holuhraun Plume Elevation Model on 6 September 2014 with a spatial resolution of 240 m per pixel. Location of the a–b and c–d elevation profiles in Fig. 4 are shown.

(s) and H is the platform height (m). The results are shown in Fig. 3. We trace two profiles on the PEM and attempt a validation with ground truth data acquired by a web camera located in Kverkfjöll, about

25 km south of the plume. The comparison between ground based and space based measurements show that the PEM values are consistent. We show the results of the validation in Fig. 4. Besides, our method

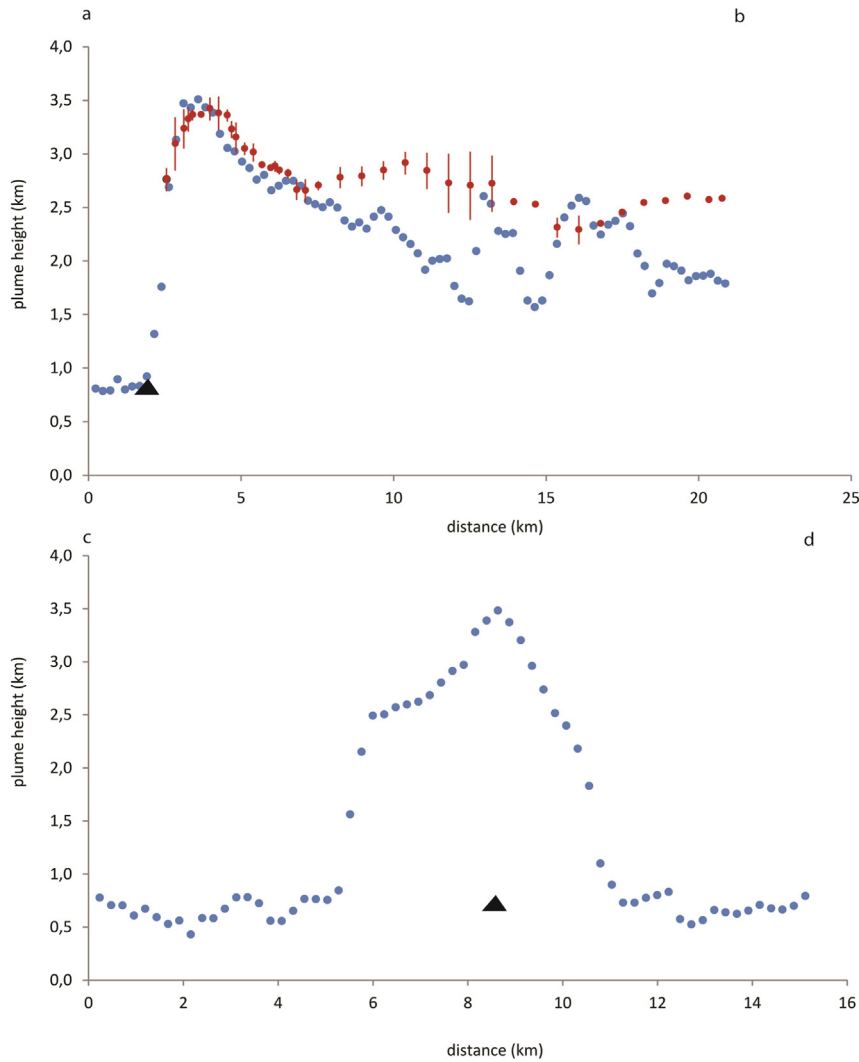


Fig. 4. Along-plume elevation profile a–b (top) and across-plume elevation profile c–d (bottom) (see location in Fig. 3). The red circles represent the average of two ground camera measurements at 12:20 UTC and 12:30 UTC that we use for validation. The red bars indicate the difference between the two ground observations). The black triangles represent the location of the eruption site. (For interpretation of the references to colour in this figure legend, the reader is referred to the web version of this article.)

provides a spatially dense measure of the plume velocity at the PEM pixel sampling (240 m)

$$v_p = O_{p2e} S / (t \cdot \cos \theta) \quad (3)$$

where v_p is the velocity of the plume along its main axis (m/s).

For the 2014 Holuhraun eruption, we estimate a velocity between 7 and 12 m/s, which is consistent with ground based observation of the plume velocity on the same day as the Landsat 8 acquisition; the wind speed of the IMO numerical weather prediction model (Harmonie) at the surface (10 m a.g.l.) at Holuhraun on 6 September 2014 at 12:00 was 8.6 m/s (Arason, Bjornsson, Petersen, Jónasdóttir, & Oddsson, 2015).

3.1. Methodological considerations

When creating images alternating panchromatic and MS stripes, two issues can arise from both geometric and radiometric origin. The first is the alignment of successive stripes (resampled at the same sampling step). In our case, we proceeded by estimating shifts on the common overlapping columns of the two stripes (e.g. panchromatic and Red) by simple image correlation. The second issue is the “calibration” of successive stripes of information acquired in different wavelengths and resolutions. We propose to proceed by adjusting the median values of successive image columns. Although the information is of different origin on the two successive stripes, the discontinuities between bands are little visible on the resulting mosaic images on land (Fig. 1).

Alternative methods could be implemented. We found that the actual resulting image product is suitable for the present application as it reduces the loss of information due to low correlation values when the correlator windows cross the borders between adjacent PAN/MS stripes.

3.1.1. Discussion on precision

In this section we discuss two sources of errors: the direct incidence of the expected inaccuracy of the offsets estimation on the height values and the incidence of the plume velocity correction. In terms of the error on the epipolar offset estimation, if we assume a theoretical correlator precision of 1/10 of pixel (Leprince et al., 2007), the resulting PEM precision (from Eq. (2) using the estimated B/H for Landsat 8) would be about 270 m. In terms of error due to insufficient velocity compensation, if we assume a theoretical correlator precision of 1/10 of pixel, the resulting error due to P2E offsets would be about 160 m. This estimation is sensitive to $\tan \theta$. As a consequence, the height measurement error will strongly increase with increasing θ . This fact yields potential extreme situations when the volcanic plume is parallel to the satellite orbit, which PEM would be impossible to compute without neglecting the plume velocity. Surely, to overcome this problem one could combine both ascending and descending paths. Secondly, we can suppose a certain dispersion of the velocities about the average direction of the plume. For our case the dispersion is between 5° and 55° with average direction of about 25°. In this case, the vertical inaccuracy of the PEM can reach up to 380 m.

In the case one neglects the plume velocity, we can deduce that an uncompensated epipolar component of the velocity δv_p might result in an error δh given by (from (2))

$$\delta h = \delta v_p \left(\frac{H}{V} \right) \quad (4)$$

which yields $\delta h \sim 100 \delta v_p$ for Landsat 8 data.

We highlight that most Low Earth Orbit (LEO) optical sensors relevant to this method share similar altitudes (600–800 km) and speeds (~7 km/s). Therefore, the ratio $\delta h / \delta v_p \sim 100$ gives an idea of the estimated error due to uncompensated plume epipolar velocity for most of the available LEO sensors. In the present test case (15 m/s

maximum P2E velocity) if we do not correct for velocity contribution, δh would be about 860 m. On the basis of the previous discussion, we are confident that our method can reasonably provide precisions in the interval 300–500 m if the velocity component is well compensated.

Our PEM is validated against in-situ independent observations in the next section.

4. Accuracy assessment with ground based measurements

A web camera was located in Kverkfjöll (64°40′30″N, 16°41′23″W, elevation 1730 m a.s.l.), about 25 km south of the vent and almost perpendicular to the plume (Arason et al., 2015). The images are available every 10 min. The camera image area was scaled by identifying seven mountains visible on the images with elevations from 741 to 1682 m a.s.l. Assuming no lens distortion and that the plume drifted into direction 80° East of North, the plume top seen in the images can be transformed to height profile above sea level vs. distance along the plume. The camera view shows the plume during the first 19 km from the eruption site.

A comparison of the plume top altitude is shown in Fig. 4, where the web camera estimates at 12:20 and 12:30 UTC are shown as red dots with their temporal variation shown as error bars. We notice that the space based heights measurements are consistent with the ground based; the accuracy is better than 150 m on the first 7 km from the eruption site.

5. Discussion and conclusions

In this article we present a method to reconstitute the Digital Elevation Model of a volcanic ash/gas plume. We apply the method to the 2014–2015 Holuhraun eruption and compare the results to ground-based observations (validation). The comparison yields a good fit, which makes us confident about the potential use of our method in remote access areas. Moreover, the method has potential for automation given that the procedure is relatively straight forward and the only input is the spaceborne imagery and associated metadata.

The produced PEM is consistent with ground observations for the first 7 km of the profile from the eruption site. The discrepancies are less than 150 m indicating that, in a range of a few km from the eruption site, our method appears to be accurate. The profile shows a height decrease starting at 3400 m over the eruption site and reaching 2500 m after 7 km. Then, between 7 km and 19 km, our PEM appears to be underestimated with respect to the ground observations by about 500 to 700 m (i.e. height values vary between 1700 m and 2500 m). A possible explanation comes from the fact that the surface of the plume is very irregular (with possible local maxima and minima for the height). Seen from the ground, the height at a given point is obtained by the highest position of the plume in the line of sight of the camera — and therefore should not correspond to a local minimum of the plume's upper surface as minima are occulted by higher elements of the plume. For the PEM, the values are extracted along a straight profile that could cross low areas of the plume occulted from the ground. That would result in an apparent underestimation. A second possible explanation can be proposed observing that far from the eruption site, the plume is more diluted, so we can see the ground through the plume on the images. A possible consequence of this, is the fact that features of the plume used in the image correlation process are deeper under the plume's upper surface than in areas where the plume is denser. We might therefore estimate heights under the upper surface instead of the upper surface itself. Finally, we cannot reject the possibility that uncertainty of the plume velocities (values and directions) could affect our PEM estimates. Based on these considerations, we recommend the use of this method only when the mean angle between plume and orbit is larger than 45° with respect to the orbit azimuth angle. If it is not the case, auxiliary information (as wind speed data) is required to improve the PEM accuracy.

We measured the plume height with respect to the surrounding topography. Therefore, it is a relative height value with respect to the lowest topography within the scene. The sea could be taken as a reference “zero” value, if the sea is present in the satellite dataset. There is a need of absolute height calibration if the scene is devoid of sea. It can be done by including local topographic data (such as a DEM).

We developed this method on FPMs sensor such as Landsat 8 in the view of the use of Sentinel-2 data, where sensors are in a similar geometry on the focal plane. But our method can be applied directly to other – more linear – push broom sensors such as the CNES SPOT family (1980–today) and Pléiades, which would improve the observation frequency, geographic coverage and number of data in archived inventories. The exploitation of these data archives would allow a study of past/present and future volcanic ash/gas columns.

Acknowledgements

The method presented in this article was constructed at BRGM. We are grateful to USGS for providing us with raw Landsat 8 images. We thank Jim Storey for the FPM's technical sheet. We thank Claudia Spinetti and Stefano Corradini at INGV, Rome. The research leading to these results received funding from the European Commission Seventh Framework Programme [FP7/2007-2013] under the MED-SUV project: grant agreement no. 308665 and under the APHORISM project: grant agreement no. 606738.

References

- Arason, P., Björnsson, H., Petersen, G.N., Jónasdóttir, E.B., & Oddsson, B. (2015). Plume height during the 2014–2015 Holuhraun volcanic eruption. *Proceedings of the European geosciences union general assembly (2015)*, EGU2015-11498, Vienna, Austria, 12–17 April 2015.
- Arason, P., Petersen, G.N., & Björnsson, H. (2011). Observations of the altitude of the volcanic plume during the eruption of Eyjafjallajökull, April–May 2010. *Earth System Science Data*, 3, 9–17. <http://dx.doi.org/10.5194/essd-3-9-2011>.
- Carboni, E., Grainger, R., Walker, J., Dudhia, A., & Siddans, R. (2012). A new scheme for sulphur dioxide retrieval from IASI measurements: Application to the Eyjafjallajökull eruption of April and May 2010. *Atmospheric Chemistry and Physics*, 12, 11417–11434.
- Corradini, S., Merucci, L., Prata, A.J., & Piscini, A. (2010). Volcanic ash and SO₂ in the 2008 Kasatochi eruption: Retrievals comparison from different IR satellite sensors. *Journal of Geophysical Research*, 115, D00L21. <http://dx.doi.org/10.1029/2009JD013634>.
- Gottelman, A., Schmidt, A., & Kristjánsson, J.E. (2015). Icelandic volcanic emissions and climate. *Nature Geoscience*, 8, 243. <http://dx.doi.org/10.1038/ngeo2376>.
- Haddadi, B., Moune, S., Sigmarsson, O., Gauthier, P.-J., & Gouhier, M. (2015). Pre-eruptive volatile and erupted gas phase characterization of the 2014 basalt of Bárðarbunga volcanic system, Iceland. *Proceedings of the European geosciences union, general assembly 2015*, EGU2015-9572, Vienna, Austria, 12–17 April.
- Hreinsdóttir, S., Sigmondsson, F., Roberts, M.J., Björnsson, H., Grapenthin, R., Arason, P., ... Óladóttir, B.A. (2014). Volcanic plume height correlated with magma pressure change at Grímsvötn volcano, Iceland. *Nature Geoscience*, 7, 214–218. <http://dx.doi.org/10.1038/ngeo2044>.
- Kääb, A., & Leprince, S. (2014). Motion detection using near-simultaneous satellite acquisitions. *Remote Sensing of Environment*, 154, 164–179.
- Kääb, A., Lamare, M., & Abrams, M. (2013). River ice flux and water velocities along a 600 km-long reach of Lena River, Siberia, from satellite stereo. *Hydrology and Earth System Sciences*, 17, 4671–4683.
- Knight, E., & Kvaran, G. (2014). Landsat-8 operational land imager design, characterization, and performance. *Remote Sensing*, 6, 10286–10305.
- Leprince, S., Barbot, S., Ayoub, F., & Avouac, J.P. (2007). Automatic and precise orthorectification, coregistration, and subpixel correlation of satellite images, application to ground deformation measurements. *IEEE Transactions on Geoscience and Remote Sensing*, 45, 6.
- Mai, S., & Latry, C. (2009). Digital elevation model computation with SPOT5 panchromatic and multispectral images using low stereoscopic angle and geometric model refinement. *Proceedings of the 2009 IEEE international geoscience and remote sensing symposium*, 12–17 July, Cape Town, South Africa.
- Massonnet, D., Giros, A., & Breton, E. (1997). Forming digital elevation models from single pass Spot data: Results on a test site in the Indian Ocean. *Proceedings of the 1997 IEEE international geoscience and remote sensing symposium*, 03–08 August, Singapore.
- Mastin, L.G., Guffanti, M., Servranckx, R., Webley, P., Barsotti, S., Dean, K., ... Waythomas, C.F. (2009). A multidisciplinary effort to assign realistic source parameters to models of volcanic ash-cloud transport and dispersion during eruptions. *Journal of Volcanology and Geothermal Research*, 186, 10–21. <http://dx.doi.org/10.1016/j.jvolgeores.2009.01.008>.
- de Michele, M., Leprince, S., Thiébot, J., Raucoules, D., & Binet, R. (2012). Direct measurement of ocean waves velocity field from a single SPOT-5 dataset. *Remote Sensing of Environment*, 119, 266–271.
- Petersen, G.N., Björnsson, H., Arason, P., & von Löwis, S. (2012). Two weather radar time series of the altitude of the volcanic plume during the May 2011 eruption of Grímsvötn, Iceland. *Earth System Science Data*, 4, 121–127. <http://dx.doi.org/10.5194/essd-4-121-2012>.
- Poupardin, A., Idier, D., de Michele, M., & Raucoules, D. (2015). Water depth inversion from a single SPOT-5 dataset. *IEEE Transactions on Geoscience and Remote Sensing PP (99)*, 1–14. <http://dx.doi.org/10.1109/TGRS.2015.2499379>.
- Robock, A. (2000). Volcanic eruptions and climate. *Reviews of Geophysics*, 38, 191–219. <http://dx.doi.org/10.1029/1998RG000054>.
- Scollo, S., Prestifilippo, M., Pecora, E., Corradini, S., Merucci, L., Spata, G., & Coltelli, M. (2014). Eruption column height estimation of the 2011–2013 Etna lava fountains. *Annales de Géophysique*, 57(2), S0214. <http://dx.doi.org/10.4401/ag-6396>.
- Sigmundsson, F., Hooper, A., Hreinsdóttir, S., Vogfjörð, K.S., Ófeigsson, B., Heimisson, E.R., ... Eibl, E.P.S. (2015). Segmented lateral dyke growth in a rifting event at Bárðarbunga volcanic system, Iceland. *Nature*, 517, 191–195. <http://dx.doi.org/10.1038/nature14111>.
- Simpson, J.J., McIntire, T., Jin, Z., & Stitt, J.R. (2000). Improved cloud top height retrieval under arbitrary viewing and illumination conditions using AVHRR data. *Remote Sensing of Environment*, 72, 95–110. [http://dx.doi.org/10.1016/S0034-4257\(99\)00095-4](http://dx.doi.org/10.1016/S0034-4257(99)00095-4).
- Sparks, R.S.J., et al. (1997). *Volcanic plumes*. Chichester: John Wiley & Sons (559 pp.).
- Spinetti, C., Barsotti, S., Neri, A., Buongiorno, M. F., Doumaz, F., & Nannipieri, L. (2013). Investigation of the complex dynamics and structure of the 2010 Eyjafjallajökull volcanic ash cloud using multispectral images and numerical simulations. *J. Geophys. Res. Atmos.*, 118. <http://dx.doi.org/10.1002/jgrd.50328>.
- Storey, J., Choate, M., & Lee, K. (2014). Landsat-8 operational land imager on-orbit geometric calibration and performance. *Remote Sensing*, 6, 11127–11152. <http://dx.doi.org/10.3390/rs6111127>.
- Urai, M. (2004). Sulphur dioxide flux estimation from volcanoes using Advanced Spaceborne Thermal Emission and Reflection Radiometer - A case study of Miyakejima volcano. *Japan. Journal of Volcanology and Geothermal Research*, 134, 1–13.
- Vadon, H. (2003). 3D navigation over merged panchromatic-multispectral high resolution SPOT5 images. *Proceedings of the 2003 ISPRS symposium. The international archives of the photogrammetry, remote sensing and spatial information sciences, Vol. XXXVI*. (pp. 5/W10).